

## New Advances in the Machining of Hard Metals using Physics-Based Modeling

Troy D. MARUSICH, Shuji USUI, Luis ZAMORANO,  
Kerry MARUSICH, Juergen LEOPOLD

*Third Wave Systems, Inc.*

7900 West 78th Street Suite 300, Minneapolis, MN USA 55439  
e-mail: sales@thirdwavesys.com

The machining of hard metals historically has been understood to be challenging and costly due to its material properties (such as titanium’s low thermal conductivity and high hardness, and nickel’s rapid work-hardening and high strength at elevated temperatures) and limited understanding in industry of the physics behind chip formation and material removal. The achievement of meaningful cycle time reductions while maintaining part quality depends on a capability to model the physics of hard metal machining operations. With the help of a validated toolpath analysis model that can predict forces at each cutter location, cycle times and scrap can be reduced and machine breakdown can be avoided, all through off-line analysis. Productivity and process efficiency can be improved through simulation, drastically reducing testing setup and machining time. Physics-based modeling technology has been identified as a cost-effective solution for identifying optimum cutting speeds, enabling researchers and manufacturers to increase material removal rates, reduce machining costs, and enhance industry expertise in hard metal machining best practices. This paper presents new advances to physics-based modeling that have been validated using experimental tests and comparisons with finite element milling simulations, used to compare different process parameters and resulting material removal rates, and successfully advance hard metal machining processes.

**Key words:** machining, process improvement, CAE software, aircraft, metal, titanium.

### 1. INTRODUCTION

In addition to complicated toolpaths inherent in airframe components, the machining of titanium alloys and other hard metals pose several challenges due to low thermal conductivity, high specific cutting power [1] and high hardness. Commercially-available verification software products provide methods to optimize such toolpaths, but do not incorporate material behavior or cutting force prediction; [2, 3]. Several empirical models to predict cutting forces in machining processes have been well documented in the literature [4–8]; and yet, these

models are not sufficient to simulate the machining of complex aerospace components utilizing five-axis toolpaths and predict forces for thousands of cutter locations and dozens of tools in a quick and efficient manner. However complicated, implementing toolpath analysis into process design can yield a wide range of benefits in many different areas. With the help of a validated five-axis toolpath analysis model that can predict forces at each cutter location, cycle times and scrap can be reduced, and machine breakdown can be avoided, all through off-line analysis.

## 2. CAD GEOMETRY AND TOOLPATH IMPORT

Prediction of cutting forces requires identification of chip thickness and local cutting edge geometry along the flutes or contour of the cutting tool. Machining houses that manufacture monolithic aerospace components use complicated five-axis toolpaths typically generated with CAM packages [9, 10]. Commercially-available verification software [2, 11] can simulate the workpiece and tool geometries in either their own proprietary formats or in more universally accepted formats such as STP and STL files. While these packages provide a capability to import CNC toolpaths in generally accepted formats (such as G-code or APT code) and import the tool and workpiece geometry, none of these packages consolidate geometric information such as chip thickness and chip shape with material behavior of high temperature alloys to give a unified predictive model which considers the geometry as well as material behavior. The force model presented in this paper utilizes its own solid modeling technology, which allows for the capture of chip loads and process parameters such as cutting speeds, radial and axial depths of cut, etc., the data from which is in turn fed into the force calculation kernel described in the next section. The output of this model is thus in terms of forces, torque and horsepower, rather than just chip load and other process parameters such as cutting speeds.

A variety of helical end mill geometries are used in the metal cutting industry. Helical cylindrical, ball end, taper helical ball, bull nosed, and special purpose end mills are widely used in aerospace, automotive and die machining industries. Similar varieties also exist in drilling geometries. While the geometry of each cutter may be different, the mechanics of the milling process at each cutting edge point are common. The model presented in this paper discretizes the cutting geometry and applies empirically generated force data based on material behavior.

## 3. FORCE PREDICTIONS

Correlating the discretized force computations to the five-axis toolpath geometry is the most critical aspect of modeling the physics of machining operations.

The methodology presented herein utilizes a semi-empirical approach to capture the material properties in the form of force data. The force data is generated experimentally as a function of several variables such as cutting speed, feed, and tool geometry (back rake, side rake angles, etc.). Figure 1 shows a representative setup used to capture the cutting force data.

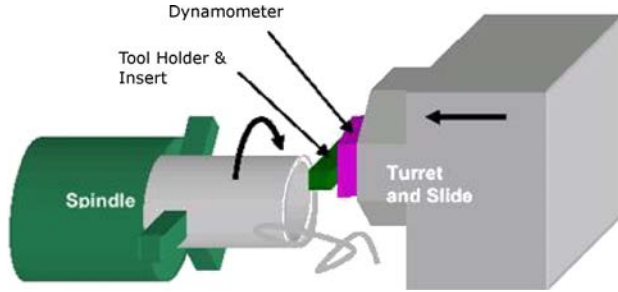


FIG. 1. Setup to capture turning force data.

Typically, force data is captured by performing tube turning measurements since these represent the simplest approach to capturing oblique cutting data. The data is captured in the form of axial, radial and tangential forces; thus for each material, tests are performed for several cutting conditions to cover the typical range of speeds, feeds and tool geometries in terms of rake angles [12].

Figure 2 shows the schematic to collect milling data using the plate dynamometer at Third Wave Systems' Productivity Center in Minneapolis, Minnesota. The force directions are captured in the coordinate system shown on the schematic, with the X-axis representing the feed direction.

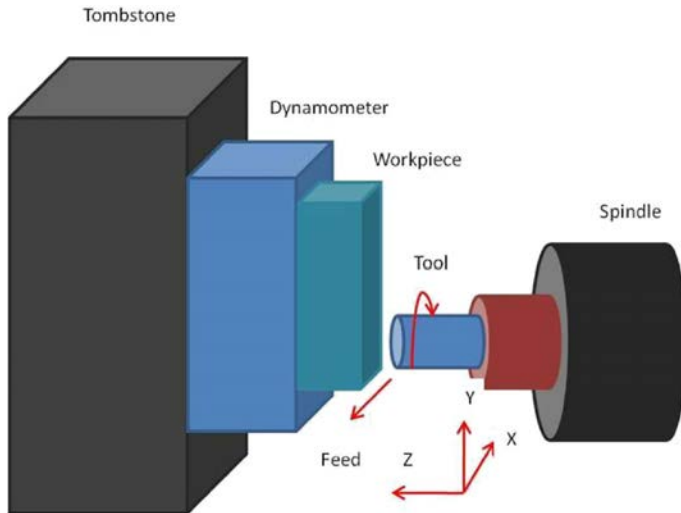


FIG. 2. Setup to capture milling force data.

## 4. EXPERIMENTAL VALIDATION

The model presented in this paper includes a material database that contains multiple materials, including commonly used aerospace and automotive materials such as titanium, nickel, aluminum, and steel alloys. Many standard tool geometries are also either readily available or can be imported in STP or STL format. This section contains a comparison between measured and predicted forces for validation from several different sources.

The first case is a validation of the force model in predicting drilling forces. A commonly used aerospace material, Ti-6Al-4V, was used as the workpiece material for modeling and testing. Forces were recorded using a Kistler 9255B table-mounted dynamometer at Third Wave's Productivity Center. A total of eight cases were machined to measure both tangential ( $F_t$ ) and normal ( $F_n$ ) forces against predicted data. Figure 3 shows the comparison of measured and predicted force values.

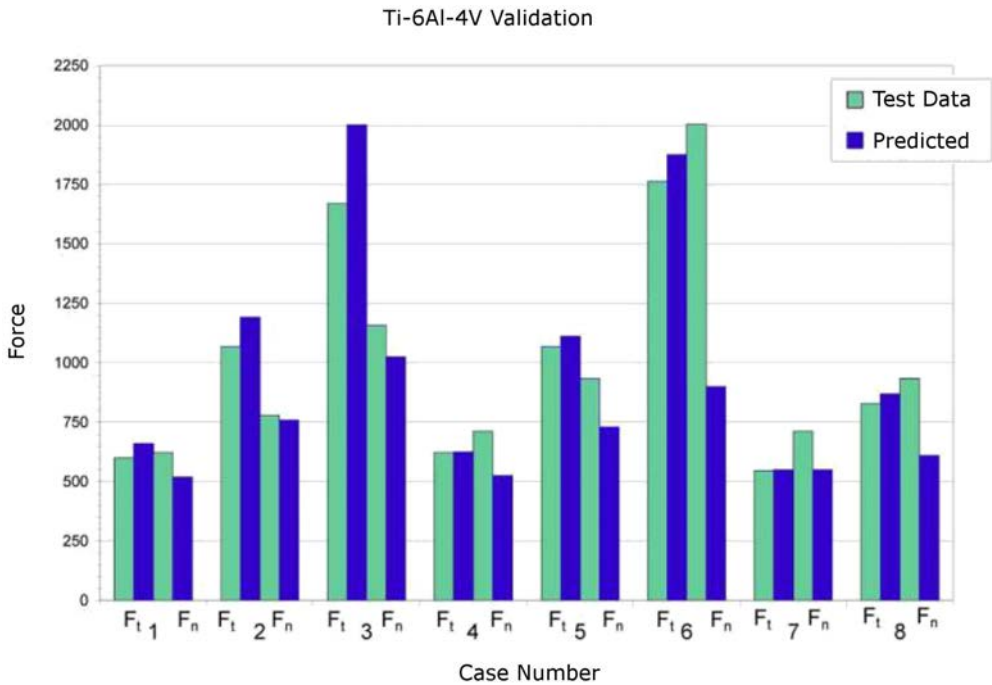


FIG. 3. Force comparison predicted by AdvantEdge FEM and measured by a dynamometer.

A second case, is validation of the force model predicting milling forces, as well as the material model prediction for chip shape. Figure 4 shows a machined chip, as well as the predicted chip behavior as modeled in AdvantEdge FEM 3D.

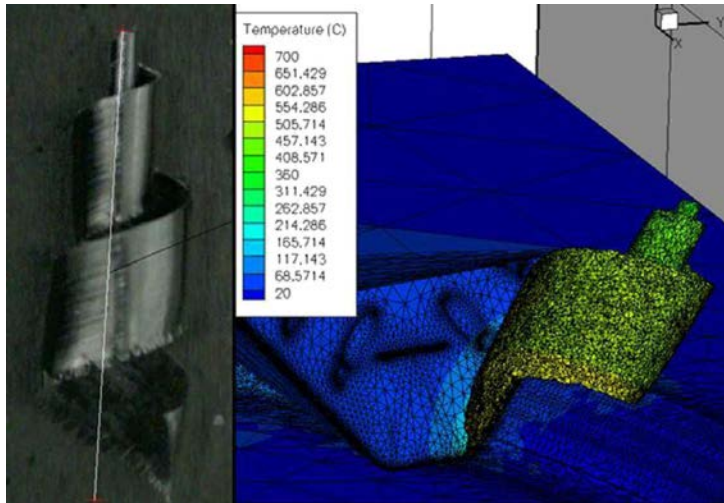


FIG. 4. Experimental test chip and predicted chip shape as modeled in AdvantEdge FEM 3D.

Figure 5 shows the predicted and measured forces of the milling operation along the X-, Y-, and Z-axes. This case was run at a speed of 146 RPM with a feed per tooth of 0.1 mm and a 40 percent radial depth of cut.

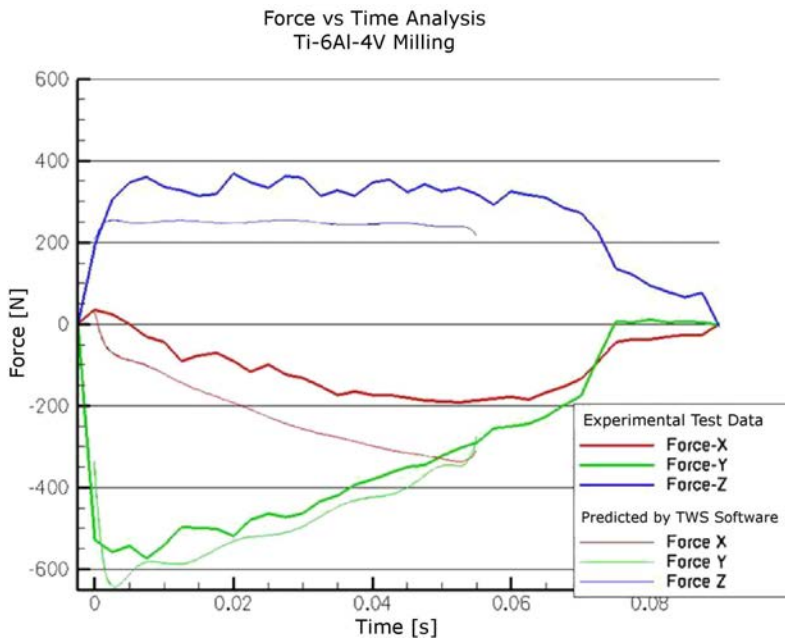


FIG. 5. Comparison of milling forces predicted by AdvantEdge FEM and measured by a dynamometer.

The third case is validation of a force model predicting power exerted on a Ti-6Al-2Sn-4Zr-2Mo workpiece. Figure 6 shows the measured spindle power labeled “TMac” compared with predictions of the force model labeled “PM” for the semi-finishing pass. Spindle power was measured using the Caron Engineering Tool Monitoring Adaptive Control-TMAC system [13]. The experimentally measured power consumption was then compared with the prediction of the force model. Instantaneous deviations between predicted and measured spindle power measurements can be primarily explained as the dynamic effects of the machine tool system that are captured experimentally.

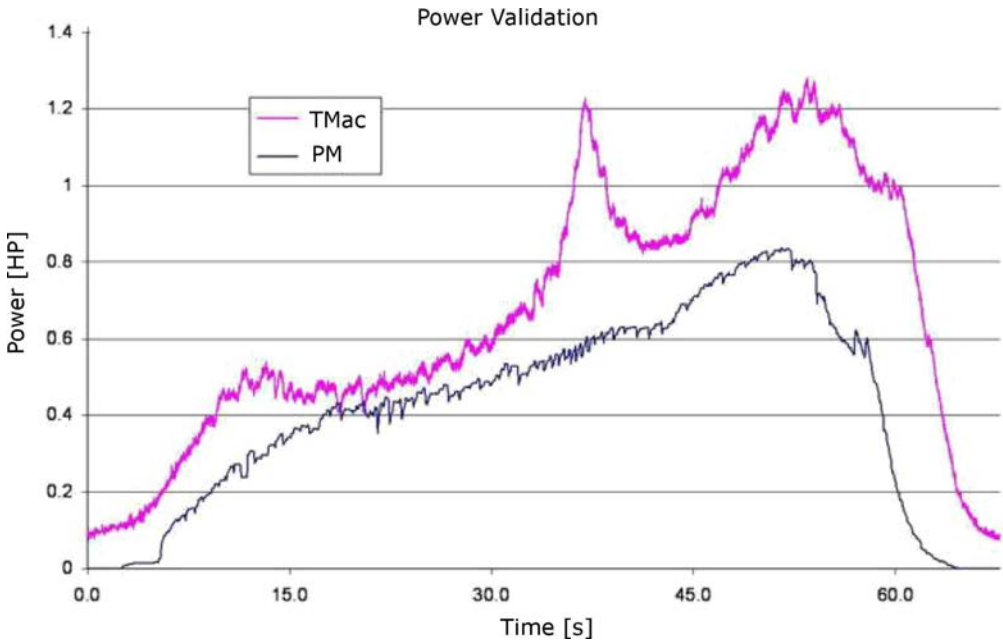


FIG. 6. Comparison of spindle power predicted by the model and measured by TMac for semi-finishing operation.

## 5. LOAD BALANCING APPROACH

With a validated model that predicts cutting forces (tool coordinate system: tangential, axial and radial; or workpiece coordinate system: X, Y and Z), torques, and spindle power, the next logical step is to utilize the model to identify areas of improvement to reduce cycle times without affecting the productivity.

Productivity improvements can be achieved by increasing the feed or speed during the cut. To increase the rate at which the tool is fed while performing a five-axis machining operation on a high temperature alloy such as a titanium or nickel alloy, material behavior and specific cutting power should be considered in addition to the tool-workpiece interactions from a purely geometric perspec-

tive. This is achieved by using the force model generated using the techniques illustrated in the “Force Predictions” section of this paper.

To increase productivity, an approach called “load balancing” was used to analyze cutting forces on the tool (e.g. tangential force) along the entire toolpath. There are instances where forces are at their peak, while at other instances along the toolpath the same tool encounters much lower cutting forces. This is primarily an outcome of tool-workpiece geometric interaction (feeds, tool orientation, and tool and workpiece geometry) and workpiece material behavior (edge and corner radius affects on the chip load and cutting forces). The entire toolpath was analyzed and cutting forces encountered by the tool and workpiece during the entire toolpath for each cutter location were computed, for all tools being called out.

In a typical multi-axis pocketing operation, a tool enters the pocket at the bottom center and gradually cuts the pocket from “inside-out” in a rectangular motion; in some CAM packages this is referred to as “outward helical” operation. The tangential force signature encountered by a tool during this pocketing operation with a workpiece material of Ti-6Al-2Sn-4Zr-2Mo is shown in Fig. 7. Maximum forces are encountered at the beginning of the pocketing operation when the tool plunged blindly into the workpiece. While cutting speeds and feeds were kept constant throughout the pocketing operation, the chip load encountered by the tool varied throughout the pocketing operation. The tool initially encountered a peak force of 9682 N; for subsequent passes, it encountered forces of 6964 N. Thus, it was possible to increase feeds in this sequence where peak tangential forces encountered by the tool were still less than the total peak tangential force encountered by this tool during the entire operation.

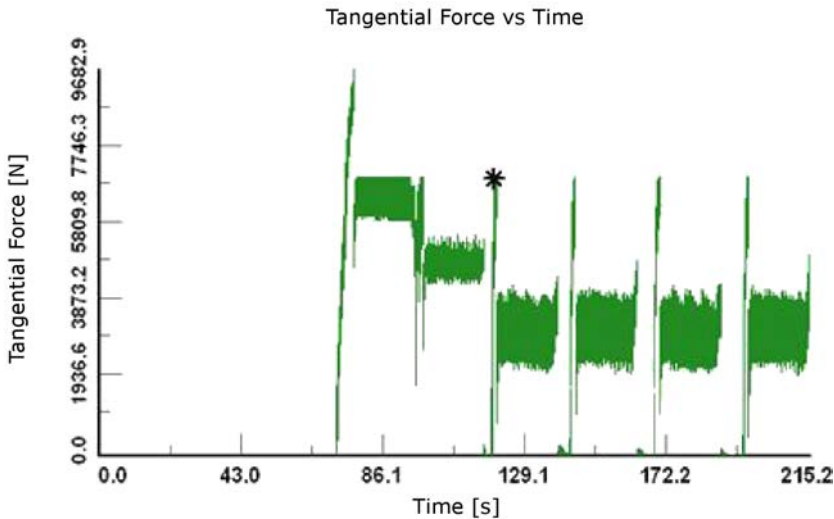


FIG. 7. Tangential force encountered by the tool.

The results, as shown in Fig. 7, are considered to be the baseline for load balancing. At each cutter location the model then compares the calculated baseline cutting forces against the upper and lower force limits set by the user. If the allowable force is higher than the currently calculated force, the feed is increased to achieve the maximum allowable force. If the allowable force is lower than the force calculated in the baseline, the feed is reduced proportionately to achieve a lowered force. The word *optimization* is used in this sense to indicate the load balancing approach; these two phrases are used interchangeably throughout the remainder of this paper.

For the baseline force signature shown in Fig. 7, if a minimum force limit of 7100 N is specified and the maximum force limit of 9682 N is maintained, the optimization yields a new sequence time of 119.8 seconds. With a baseline sequence time of 215.2 seconds, this means an approximate savings of 44 percent, as shown in Fig. 8. Notice that the peak force encountered by the tool did not exceed the original maximum value of 9682 N. It is important to note that during load balancing, spindle speeds were kept unchanged.

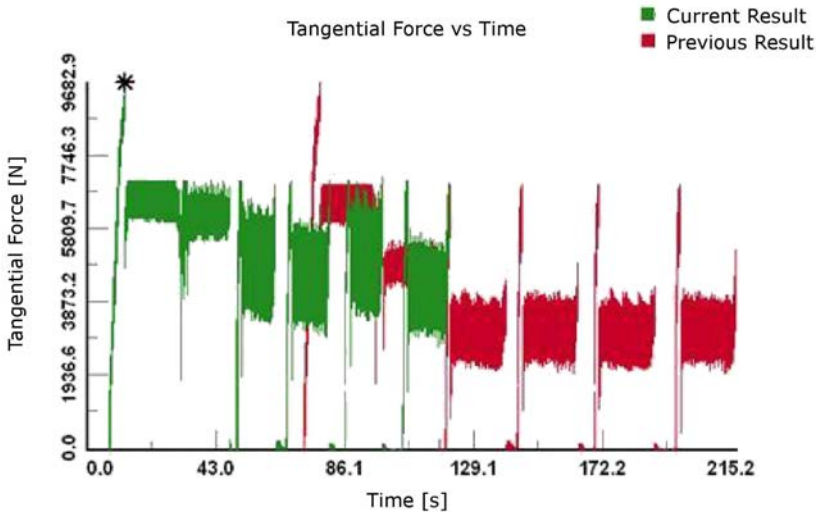


FIG. 8. Comparison of baseline (previous result) and optimized (current result) force signatures.

## 6. APPLICATION

Consider an aerospace part machined from a Ti-6Al-4V rectangular plate with dimensions of 285 mm  $\times$  160 mm  $\times$  55 mm. The minimum thickness of the walls is 7 mm and the lowest feed/tooth is 0.025 mm/tooth. Thus this simulation requires a scale difference of 285 mm/0.025 mm – 11360X – to represent its longest to shortest length scales and capture several magnitude length scales in between. The part calls in four different tools to perform several pocketing

operations on the rectangular plate to achieve the final part geometry. Figure 9 shows the finished workpiece geometry along with the toolpath.

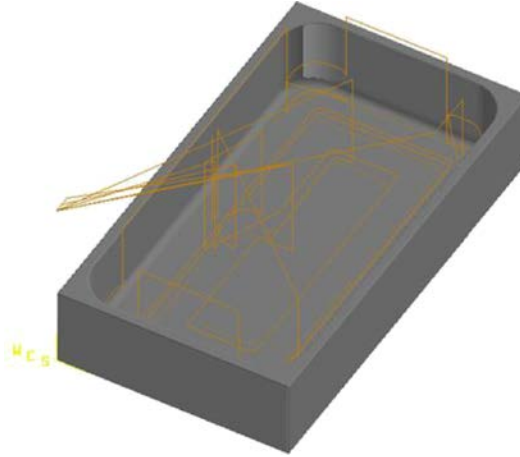


FIG. 9. Aerospace pocket component.

For the sake of the current example, only representative operations by each tool were considered; thus, the total cycle time of the entire part was only a fraction of total cycle time. Each tool encountered different maximum and minimum chip loads and correspondingly different maximum and minimum cutting forces. Figure 10 shows the baseline results noted as “previous results” (tangen-

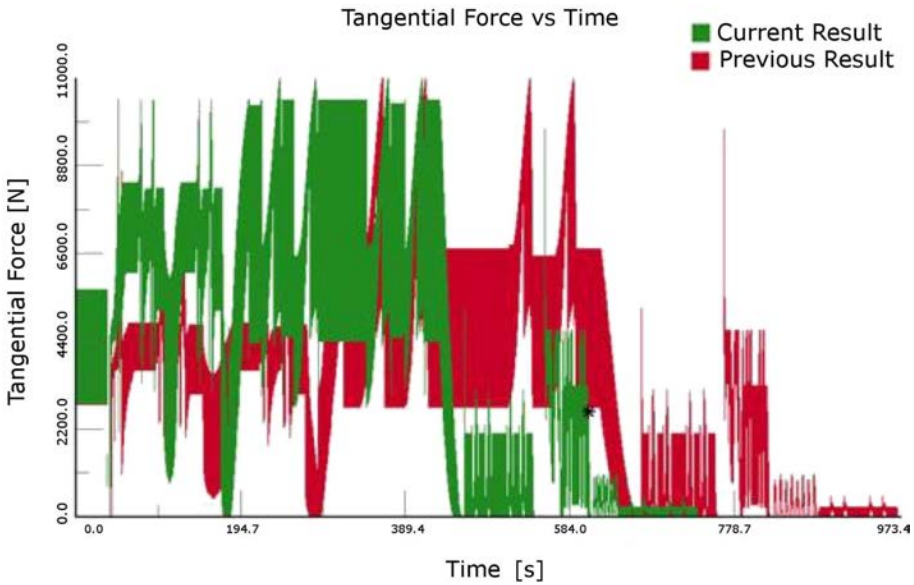


FIG. 10. Comparison of baseline and optimized force signature.

tial forces before load balancing) as well as optimized results noted as “current results” (tangential forces after load balancing.) The total “in cut” machining cycle time for all four tools was reduced from 973 seconds to 734 seconds, approximately a 25 percent improvement in productivity. It is important to note that the peak forces encountered by each tool were different and, correspondingly, the limits of tangential forces used to balance the loads on each tool were set separately.

The example above utilized only changes to the cutting feeds. Other approaches to further improve productivity, such as additional analysis using different tool geometries or toolpaths, are beyond the scope of this paper, yet yield even higher savings in cycle times using the same predictive force model presented here.

## 7. CONCLUSION

An accurate prediction of five-axis machining process behavior, including cutting forces and horsepower consumption, is necessary for the understanding of the process and for subsequent improvements to be made. It is possible to predict forces over the entire toolpath using analytical and numerical techniques to extend an empirical database to generalized cutting conditions. This semi-empirical model is able to predict torque and cutting forces encountered by the tool for drilling and milling operations. Using the same model, it is also possible to achieve a tangible reduction of cycle time while maintaining part quality.

## REFERENCES

1. STEPHENSON D.A., AGAPIOU J.S., *Metal Cutting Theory and Practice*, Second Edition, CRC, Boca Raton, FL, 19, 2006.
2. CG Tech, Vericut, [www.cgtech.com/usa/products/](http://www.cgtech.com/usa/products/).
3. DIEHL S.A., *TrueMill<sup>®</sup> White Paper*, [www.surfware.com/truemill\\_toolpath\\_strategies.aspx](http://www.surfware.com/truemill_toolpath_strategies.aspx)
4. DEVOR R.E., KLINE W.A., ZDEBLICK W.J., *A Mechanistic Model for the Force System in End Milling with Application to Machining Airframe Structures*, Proceedings of the 8th North American Manufacturing Research, 297, 1980.
5. NAKAYAMA K., ARAI M., TAKEI K., *Semi-empirical equations for three components of resultant cutting force*, Annals of the CIRP, **32**, 1, 33–35, 1983.
6. BROWN C.A., *A Practical Method for Estimating Forces from Tool-chip Contact Area*, Annals of the CIRP, **32**, 1, 91–95, 1983.
7. STEPHENSON D.A., AGAPIOU J.S., *Calculation of Main Cutting Edge Forces and Torque for Drills with Arbitrary Point Geometries*, International Journal of Machine Tool Manufacturing, **32**, 4, 521–538, 1992.

8. SRINIVAS B.K., *The Forces in Turning*, SME Technical Paper, MR82-947, 1982.
9. Siemens PLM Software, NX CAM, [www.plm.automation.siemens.com/en\\_us/products/nx/machining/machining/index.shtml](http://www.plm.automation.siemens.com/en_us/products/nx/machining/machining/index.shtml).
10. Dassault Systems, CATIA, [www.3ds.com/products/catia/catia-discovery/](http://www.3ds.com/products/catia/catia-discovery/).
11. Predator Software Inc., Predator SDK, [www.predator-software.com/virtualcnc.htm](http://www.predator-software.com/virtualcnc.htm).
12. STEPHENSON D.A., BANDOPADHYAY P., *Process-Independent Force Characterization for Metal Cutting Simulation*, Transactions of the ASME, **119**, 1997.
13. Caron Engineering, Inc., [www.caron-eng.com/](http://www.caron-eng.com/).

*Received May 10, 2011; revised version January 4, 2013.*

---